Engineering in Life Sciences

Eng. Life Sci. **2016**, *16*, 762–768 www.els-journal.com

Mamta Chauhan*
Ragothaman M. Yennamalli*
Vijay Kumar Garlapati

Department of Biotechnology and Bioinformatics, Jaypee University of Information Technology, Waknaghat, Himachal Pradesh, India

Research Article

Biochemical characterization and molecular modeling of a unique lipase from *Staphylococcus arlettae* JPBW-1

A three-step purification of a unique lipase with halo-, solvent-, detergent-, and thermo-tolerance from *Staphylococcus arlettae* JPBW-1 gave raise to a 27-fold purification with a specific activity of 32.5 U/mg. The molecular weight of the purified lipase was estimated to be 45 kDa using SDS–PAGE, and its amino acid sequence was characterized using MALDI-TOF-MS analysis. The sequence obtained from MALDI-TOF-MS showed significant similarity with the capsular polysaccharide biosynthesis protein (CapD) of *Staphylococcus aureus* through comparative modeling approach using ROBETTA server. Identification of responsible fragments for homodimer formation was performed using comparative modeling and substrate binding domain through C-terminus matching of this new lipase with the CapD of *Staphylococcus aureus* was executed. Thus, the experimental coupled molecular modeling postulated a structure–activity relationship of lipase from *S. arlettae* JPBW-1, a potential candidate for detergent, leather, pulp, and paper industries.

Keywords: Lipase / MALDI-TOF / Molecular modeling / Purification / *Staphylococcus arlettae* JPBW-1

Additional supporting information may be found in the online version of this article at the publisher's web-site

Received: March 20, 2016; *revised:* April 13, 2016; *accepted:* May 9, 2016

DOI: 10.1002/elsc.201600074

1 Introduction

The industrial enzymes market was valued at USD 4.2 Billion in 2014 and is projected to grow at a CAGR of 7.0% from 2015 to 2020. The market segmentation of detergent enzymes such as lipases, proteases is about 29% of the total industrial enzymes share. The global lipase market is projected to reach USD590.5 Million by 2020, at a CAGR of 6.5% between 2015 and 2020 as a result of rising awareness of the numerous applications of microbial lipases among the livestock producers in developing regions, such as Asia-Pacific and Latin America. (http://www.marketsandmarkets.com/Market-Reports/lipase-market-205981206.html). Microbial lipases (triacylglycerol acyl hydrolases, EC 3.1.1.3) are hydrolases with the natural function of catalyzing the hydrolysis of esters at the oil–water interface. The microbial lipases differ from each other in terms of activity, fatty acid specificity, and properties [1]. Microbial extracellular lipases are the preferred enzymes in the pharmaceutical, food, cosmetic, detergent, biofuel sectors due to its rigidity, stereo-, and substrate-specificities [2, 3].

The multifold industrial applications of microbial lipases from the unique environmental niches have been attributed to their stability under harsh industrial conditions, catalytic diversity, and genetic manipulation amenability with broad substrate specificity [4]. Although, many microbial lipases have been commercialized for different industrial applications, the thrust for extremophilic lipases that can work under harsh industrial conditions persists [5–7]. Microbial lipases are usually purified based on its subsequent end usage through a combination of precipitation and chromatography techniques. Basheer *et al.* reported

Correspondence: Dr. Vijay Kumar Garlapati, (shanepati @gmail.com), Department of Biotechnology and Bioinformatics, Jaypee University of Information Technology, Waknaghat, Himachal Pradesh 173234, India

Abbreviations: BLAST, Basic Local Alignment Search Tool; **BSA**, Bovine Serum Albumin; **CAGR**, compound annual growth rate; **DEAE**, diethylaminoethyl; **EDTA**, ethylenediaminetetraaceticacid; **kDa**, kilodalton; **MSDB**, Mascot Search Database; **NADB**, Nucleic Acid Database; **NCBI nr**, National Center for Biotechnology Information non-redundant; **NEK**, nucleotide sequences-encoding kinase; **PDB**, Protein Data Bank; **UniProt**, Universal Protein Resource

*Both authors contributed equally

a lipase purification fold of 30.2 through a two-step purification of anion-exchange chromatography (DEAE Sepharose) and gel filtration chromatography (Superdex G-100) [8]. A three-step purification scheme (ammonium sulphate precipitation, phenyl sepharose, sephacryl-100 gel chromatography) brought about a 149 purification fold in case of extracellular lipase from *Aspergillus niger* NCIM 1207 [9].

Detergent industries are looking for novel lipases with thermo- and detergent-tolerate properties to withstand the washing cycle temperatures and to work under harsh detergent formulation ingredients. We had earlier reported the lipase obtained from *Staphylococcus arlettae* as having properties those have desired traits for industrial application [10]. More specifically, this lipase isolated from a rock salt mine had exhibited, solvent-tolerance (in benzene, xylene, toluene, n-hexane, methanol, and ethanol up to 30% (v/v)), thermostability (significantly active at temperatures ranging from 30–90°C), and detergent resistant (enhanced activity in presence of Tween-80, Tween-40, and EDTA) along with the halo- tolerance (up to 20%) [10].

In the absence of protein structures obtained from X-ray or NMR techniques, molecular modeling methods deliver a quicker alternative to understanding the structure and function of protein. With the availability of genomic sequences coupled with computational methods that have higher accuracy and sensitivity, generating a protein's structure from its sequence has become a routine bioinformatics analysis for biologists [11]. The most frequently used method is comparative modeling (also known as homology modeling or template-based modeling) of protein structure. The other less frequently used method is *de novo* or *ab-initio* modeling of protein structure. While the former requires a suitable structure as a template (preferably a sequence identity of above 50%), the latter builds the protein structure using first principles or other techniques that do not rely upon sequence-level homology [11].

Our earlier report consisted of partially purified lipase, and in this paper, we present the multifold purification step coupled with molecular modeling analysis that exhibits unique traits that are industrially relevant.

2 Materials and methods

2.1 Microorganism and chemicals

The bacterial strain, *S. arlettae* JPBW-1 used in this study, was isolated from the rock salt mine in Darang, Himachal Pradesh, India and was identified by 16S rRNA analysis [10]. *Staphylococcus arlettae* JPBW-1 was cultured in Luria-Bertani (LB) medium (pH 7.0) consisting of the casein enzymic hydrolysate (10 g/L), yeast extract (5 g/L), and sodium chloride (10 g/L). *p*-Nitrophenyl palmitate, sodium dodecyl sulphate (SDS) standard protein markers, Coomassie brilliant blue R-250, bromophenol blue, DEAE sepharose, Sephacryl S-200 matrices were procured from Sigma Chemical Company, USA. All the other chemicals used were of analytical and high purity grade available locally.

2.2 Lipase production

Submerged fermentation was carried out by seeding the spore suspension (50 mL) in Erlenmeyer flasks (1000 mL) containing 500 mL of the LB medium, supplemented with soybean oil (12 % v/v). The flasks were incubated at 35°C under agitation (100 rpm) for 3 h. After 3-h incubation, the fermentation medium was harvested by centrifugation at 6314 × *g* for 10 min at 4°C [10]. The supernatant was collected for estimation of lipase activity and protein.

2.3 Lipase assay and protein estimation

Lipase activity was estimated using *p*-nitrophenyl palmitate (*p*-NPP) as the substrate [12]. One enzyme unit was defined as the amount of lipase that liberates 1 μmol of *p*-nitrophenol per minute under the assay conditions. The protein content of the cell-free supernatant was determined by a modified Lowry method using BSA as a standard [13].

2.4 Purification of *S. arlettae* lipase

2.4.1 Ammonium sulphate precipitation

The initial purification of cell-free culture supernatant was started with the ammonium sulphate precipitation (60%). The obtained pellet after centrifugation (30 min at 8000 rpm) was dissolved in 10 mL of buffer (50 mM Tris-HCl, pH 8.0) [14]. Partially purified lipase was further subjected to dialysis against 50 mM Tris–HCl buffer (pH 8.0) overnight.

2.4.2 Ion exchange chromatography

The lipase obtained after dialysis was directly applied on a DEAE-Sepharose column (15×1.6 cm id, Bio-Rad Laboratories, USA), previously equilibrated with 50 mM Tris–HCl buffer, pH 8. The exchanged material was eluted with a linear gradient of NaCl (ranging from 0.0 to 0.5M), prepared in the same buffer at a flow rate of 60 mL/h and collected in 3 mL fractions with the help of AKTA Prime Plus (GE Life Sciences, USA). Fractions coming under the peak were pooled, dialyzed, and then activity was measured through *p*-NPP assay. High specific activity fractions were pooled, concentrated by ammonium sulphate precipitation for further subsequent purification steps (Supporting Information Fig. 1).

2.4.3 Gel filtration chromatography

The concentrated lipase from IEC step was further passed through Sephacryl S-200 column (93 cm × 1.6 cm id, Bio-Rad Laboratories, USA) (equilibrated with Tris–HCl buffer, 50 mM, pH 8.0) with a flow rate of 30 mL/h. Three milliliter fractions were collected with the aid of AKTA Prime Plus (GE Life Sciences, USA) and screened for lipase activities. The fractions with lipase activity were further pooled for subsequent analysis (Supporting Information Fig. 2).

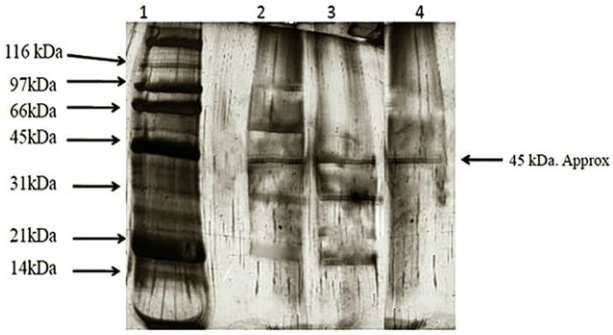

Figure 1. SDS-PAGE analysis on the purified enzyme. Lane 1: molecular weight markers; Lane 2: crude enzyme; Lane 3: partially purified lipase (after DEAE-Sepharose column chromatography); Lane 4: purified lipase (after Sephacryl S-200 column chromatography).

2.5 Molecular weight determination through SDS-PAGE

The molecular mass of the denatured protein was investigated using SDS-PAGE (Amresco, USA). An SDS-10 % polyacrylamide gel was prepared according to the modified Laemmli, 1970 method [15] (Fig. 1). Reference proteins (Biorad 161–0317) for molecular mass determination of the microbial lipase used in the present study were lysozyme (14.4 kDa), Trypsin inhibitor (21.5 kDa), carbonic anhydrase 31 kDa), ovalbumin (45 kDa), bovine serum albumin (66.2 kDa), Phosphorylase b (97.4 kDa), β-galactosidase (116 kDa), and myosin (200 kDa). Protein bands were visualized by silver staining.

2.6 Peptide mass fingerprinting by MALDI-TOF-MS

Premixed matrix (0.5–1.0 μL) was loaded on spots (mixed sample and matrix solutions in 1:2 ratios) present on the sample stage then allowed the mixture to air-dry at room temperature (< 5 mins). The air-dried mixture was washed with TFA (0.1 %), analyzed by Ultraflex TOF/TOF mass spectrometer (Bruker Daltonics, Bremen, Germany), which was calibrated by peptide calibration standard II (Bruker). An acquired mass spectrum with a ~6000 (FWHM) resolution was sufficient to identify the digested peptide (Fig. 2). The obtained mass/charge (*m/z*) spectra were searched in Mascot search engine (http://www.matrixscience.com) using all the three databases, namely MSDB, Swiss-Prot, NCBI nr by assuming peptides were monoisotopic, oxidized at methionine residues, carbamidomethylated at cysteine residues. A peptide mass tolerance of 1.2 kDa was used for peptide mass fingerprinting.

2.7 Bioinformatics analysis and de novo structure prediction

The MALDI-TOF data obtained were matched using the Mascot analysis search engine (http://www.matrixscience.com). The highest match with the highest score (Mass of 67633 Da, Mascot score of 53, *E*-value of 0.13) was with capsular polysaccharide biosynthesis protein (CapD) from *Staphylococcus aureus* (UniProt id: P39853 (CAPD_STAAU) and Genbank accession id: AAA64643.1). A comparative modeling approach was performed to predict the 3D structure of *S.aureus* CapD (599 residues). By submitting the sequence to ROBETTA server (http://robetta.bakerlab.org), two regions of the protein were modeled separately and the final models were obtained by combining both the results [16] of Ginzu domain prediction algorithm. More specifically, the individual domains predicted are assembled in an iterative process starting from the N-terminus. The final models are given to the user after a Monte Carlo repacking of side chains is performed, where backbone-dependent side-chain rotamer library is used as refinement of the final structure [16]. Using the structure obtained from ROBETTA, structural analysis was performed, where the results of MALDI-TOF-MS was mapped to identify potential functional sites. Apart from mapping the peptide fragments to the modeled structure, we attempted to map the putative catalytic triad of the lipase onto the CapD protein structure. Also, to identify putative domains that most likely aid in substrate binding, structural superposition analysis was done with the lipase from *Chromobacterium viscosum*. The resultant superposed structures were analyzed for identification of domain that possibly aides in substrate binding in CapD.

3 Results and discussion

3.1 Purification of lipase

The lipase extract from *S. arlettae* has been subjected to a three-step purification involving ammonium sulphate precipitation, ion exchange (DEAE sepharose) chromatography, and gel filtration (Sephadex S-200) (Supporting Information Figs. 1 and 2). The enzyme extract was precipitated by ammonium sulphate for concentration. The precipitate was dissolved in a minimum volume of Tris-HCl buffer (pH 8.0) then dialysis was done in order to remove any salt concentration. Then it was loaded onto the pre-equilibrated DEAE-Sepharose column. The pooled concentrated lipase active fractions from DEAE-Sepharose were subjected to gel filtration chromatography, which brought about 27 purification fold with a specific activity of 32.5 U/mg (using *p-NPP* as a substrate) and yield of 11% (Table 1). The homogeneity of lipase was confirmed through the presence of a single band of protein at 10% SDS-PAGE (Fig. 1). A molecular weight of 45 kDa was estimated for *S. arlettae* lipase (comprising ~410 residues). The molecular weight of *S. arlettae* lipase was similar to that obtained from *Mucor hiemalis* (45 kDa) and *S. aureus* lipase was estimated to be 45 kDa by SDS-PAGE [17, 18]. Most microbial lipases have a molecular weight ranging from 19 to 60 kDa and are classified as belonging to the α/β hydrolase family with an active site formed by the catalytic triad of Ser, Asp, or Glu, and His residues [1, 2].

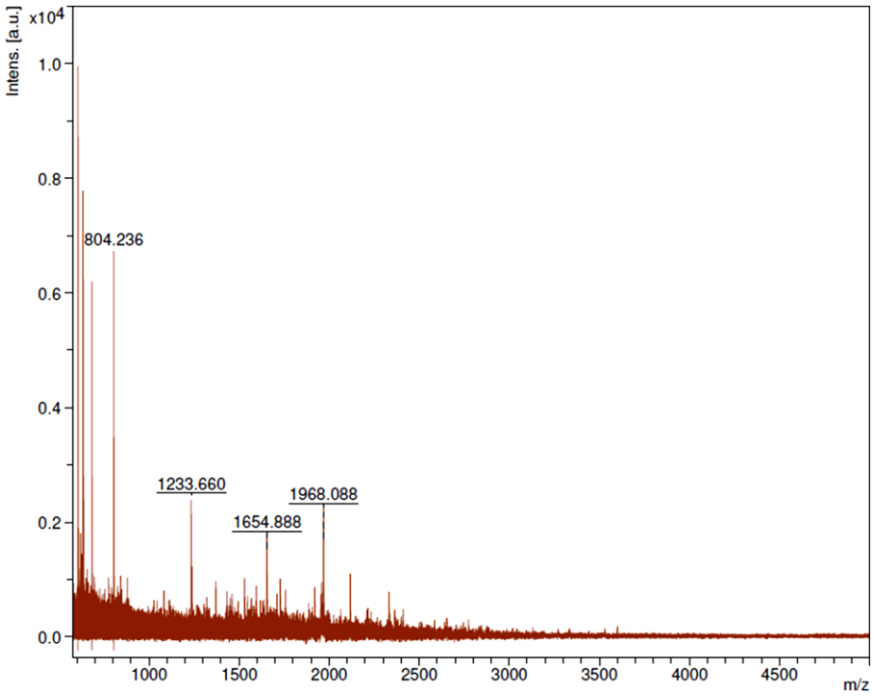

Figure 2. MALDI-TOF-MS results of *S. arlettae* JPBW1 lipase. The Y axis is labeled as relative intensity. This is the intensity relative to the tallest peak in the spectrum with the tallest peak set to 100%. The X axis is labeled *m/z*, mass divided by charge.

Table 1. Purification of lipase from *Staphylococcus arlettae*

Step	Total units (U)	Total protein (mg)	Specific activity (U/mg)	Purification fold	Recovery (100%)
Crude enzyme	354	299.48	1.18	1	100
$(NH_4)_2SO_4$ precipitation	110	25	4.40	3.72	31.07
DEAE Sepharose	88	5.2	17.60	14	24
Sephacryl S200	39	1.2	32.50	27	11

3.2 Peptide mass fingerprinting by MALDI-TOF-MS

Peptide-mass fingerprinting was carried out, and the query was searched against the MSDB, Swissport, and NCBI databases showed that the query sequence shared a significant similarity (*E* value of 0.13 and a MASCOT score of 53) with CapD protein of *S.aureus* (Table 2). It has to be noted here that a higher score in MASCOT means that more peptides were identified from a particular protein. There were six queries that matched to CapD sequence with four hits at the C- terminus region, and two hits at the N-terminus region. The Genbank entry of CapD protein (sometimes referred as Cap1D is involved in the biosynthesis of Type 1 capsular polysaccharide biosynthesis) has functional regions annotated, which are listed in Table 3.

3.3 Comparative structure modeling

The three-dimensional (3D) structure facilitates the structural analysis and characterization of any protein, in this case, an extremophilic lipase. Comparative modeling based protein structure prediction of protein structure is a quicker strategy of structural analysis as compared to X-Ray diffraction or NMR. However, a limitation of comparative modeling is the availability of a homologous template with a significant sequence identity (at least >60%) and maximum query coverage in the alignment. Since there are no known structures available for the *S. aureus* enzyme; BLAST against the PDB database was performed to identify homologous structures. However, BLAST results indicated homologous structures ranging from 24 to 37% sequence identity and a query coverage ranging from 11 to 52%, only for the matched regions (Supporting Information Table 1). It was observed that the matched regions belonged only to the C-terminus of CapD, where the domain has been reported in Conserved Domain Database (http://www.ncbi.nlm.nih.gov/Structure/cdd/cdd.shtml) as belonging to the NAD-binding Rossmann superfamily, and the query was predicted to have multiple domains. Rossmann fold NAD(P) superfamily, in general, is a large family of proteins that share a Rossmann-fold NAD(P)H/NAD(P)(+) binding (NADB) domain, where the NADB domain is found in numerous dehydrogenases of metabolic pathways such as glycolysis, and many other redox enzymes.

While we do not have the full sequence of *S. arlettae*'s lipase we undertook the structural determination of its homolog CapD from *S. aureus*. Since both proteins belong to the Staphylococcus genus and the lipase and CapD have significant homology (from

Table 2. MALDI-TOF-MS results of *Staphylococcus arlettae* lipase highlighting the highest scored matched to the Capsular polysaccharide protein (CapD) from *Staphylococcus aureus* as observed from the Mascot results

CAPD_STAAU (Uniprot id: P39853) (Mass 67633, Score 53, Expect 0.13, Queries matched: 6) Capsular polysaccharide biosynthesis protein CapD – *Staphylococcus aureus*

Observed	Mr (expt)	Mr (calc)	Ppm	Start	End	Miss	Peptide
606.1202	605.1130	605.3384	−372.47	2	7	0	M.TSISAK.L
634.1580	633.1507	633.3122	−255.02	304	308	0	K.FDPQK.I
636.1400	635.1327	635.2697	−215.60	162	166	0	R.SQDMR.M
1728.9579	1727.9507	1727.8440	61.7	68	82	0	R.AWEYASVSELMSVLK.A + Oxidation (M)
1968.0876	1967.0803	1967.9371	−435.36	462	479	0	K.NQIESGGPVTVTHPEMTR.Y + Oxidation (M)
2332.1863	2331.1790	2330.1881	425	349	368	0	R.ILEVMNEFKPYAVYHAAHK.H

There were six queries matched with a total score of 53, where the peptide fragments are compared with the experimentally observed and calculated molecular weight.

No match to: 580.1128, 582.0972, 620.1204, 622.1316, 628.1249, 635.1081, 656.1343, 684.1343, 684.1266, 686.1478, 776.1977, 804.2362, 881.2488, 1082.5731, 1224.6504, 1233.6603, 1236.7476, 1238.7191, 1304.6989, 1319.6935, 1370.7605, 1431.8289, 1442.7991, 1450.8005, 1461.8289, 1475.8046, 1494.7859, 1529.8413, 1531.7803, 1547.8704, 1567.8151, 1581.8020, 1595.8856, 1617.8937, 1631.8592, 1638.8531, 1654.8876, 1709.8668, 1757.9134, 1885.9831, 1920.0053, 1958.0247, 2117.1808, 2210.1203, 2215.0886, 2233.1035, 2337.1829, 2363.2056, 2399.1230, 2410.2460, 2651.3409, 2772.4834, 3270.7164, 3528.7614, 3598.8404

Table 3. Sequence annotation of *Staphylococcus aureus* CapD protein (Genbank accession id: AAA64643.1) highlighting the residues that have validated functions assigned

Residues	Functional annotation
Ile12 – His571	NDP-sugar epimerase, includes UDP-GlcNAc-inverting 4,6-dehydratase FlaA1 and capsular polysaccharide
Thr280 - Arg566	biosynthesis protein EpsC UDP-Glcnac (UDP-linked N-acetylglucosamine) inverting 4,6-dehydratase
Gly288, Gly290-Ile293, Gly313, His314, Ala341-Val343, Ala364-Ala366, Lys368, Asn383, Ile406, Lys422, Phe446-Val449, Ser452, Arg453	NAD(P) binding site
His314, Glu316, Tyr320, Gln324, Val339-Asp342, Asn345, Arg348, Ala366-His369, Leu372, Asn376, Glu379, Arg382, Arg453, Gly454, Leu459	Homodimer interface
Lys368, Thr408-Lys410, Met418, Gly447, Asn448, Gly454-Val456, Leu459, Phe460, Thr471-Thr473, Met477, Arg479, Ile514, Arg540, Glu543	Substrate binding site
Asn384, Thr408, Met418, Lys422	Active site

MALDI-TOF-MS results), we postulate that there is a high likelihood of shared structural similarity, even though their functional roles are albeit different. An orthogonal approach of structure prediction is using ROBETTA server, where the comparative modeling algorithm is different from the textbook method of comparative modeling (also known as homology modeling). In the absence of a good template, ROBETTA has been reported to work better to generate 3D protein models. In Critical Assessment of Structure Prediction (CASP) evaluations ROBETTA has been ranked among the top 'Fully Automated' methods [16]. Specifically, ROBETTA uses a domain prediction method called Ginzu, which uses a six-step search using BLAST, PSI-BLAST, FFAS03, and 3D-Jury (in that same order) to obtain sequences from homologous sequences that have an experimentally determined structure [16].

ROBETTA predicted the final structure of CapD by segmenting it as two domains, where residues Met1-Asn63 was modeled using the PDB structure 1NEK (D chain) as the potential template and residues Leu64-Arg599 was modeled using the PDB structure 4WKG (F chain) as the potential template (The model has been submitted to www.modelarchive.org, a repository similar to PDB for structures derived using computational methods (DOI: http://www.modelarchive.org/doi/10.5452/maaahh4). ROBETTA also give a confidence score for the domains for which the structure is built. Thus, for the model built for residues Met1-Asn63 had a score of 0.2487 and for the model built for residues Leu64-Arg599 had a score of 0.5124, which indicates that the C-terminus of CapD is a relatively more accurate structure that will be built using the de novo approach. The C-terminus region of CapD has been annotated as UDP-GlcNAc-inverting

Eng. Life Sci. **2016**, *16*, 762–768

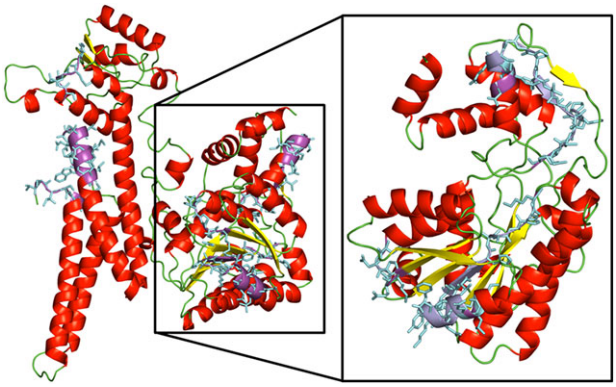

Figure 3. ROBETTA comparative modeling. Structure of the significant hit from MALDI-TOF-MS results, *S. aureus* CapD protein (involved in Type I capsular polysaccharide biosynthesis), modeled using ROBETTA automated protein structure prediction server, shown in cartoon representation. The six sequence matches are highlighted are shown in magenta, with their side chains shown in sticks representation and colored cyan. The C-terminus region is shown in the inset (rotated for clarity). There are three sequences of *S. arlettae* are mapped on to CapD protein, where two are in the Rossmann fold and the third in the putative lid-like structure. Image was made using PyMOL [21].

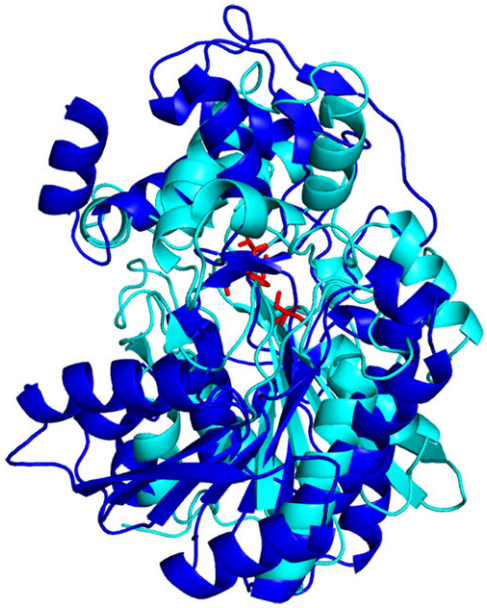

Figure 4. Structural superposition of C-terminus of CapD with *Chromobacterium viscosum* lipase. Both proteins as shown in cartoon representation, where CapD is shown in blue color and *C. viscosum* lipase is shown in cyan. The active site residues of the latter is shown as sticks and colored red. Image was made using PyMOL [21].

4,6-dehydratase (Table 3) and it has the quintessential α/β Rossmann fold. This correlates well with the secondary structure prediction of CapD from ROBETTA (using PsiPred prediction [19], which predicted the protein to belong to the α/β class of protein quaternary structure.

The C-terminus (Fig. 3 inset) modeled into a Rossmann fold (eight beta strands sandwiched between alpha helices) are made from residue Glu271 to Arg599. In Fig. 3, the amino acid sequences of *S. arlettae* JPBW-1 lipase obtained from MALDI-TOF-MS have been mapped on CapD of *S. aureus* (highlighted in magenta), and it can be clearly seen that two sequences are part of the Rossmann fold-domain. While there is no experimental evidence of NAD(P) binding to lipase, there is an NAD(P) binding region annotated for CapD (residues 288, 290–293, 313–314, 341–343, 364–366, 368, 383, 406, 422, 446–449, 452–453) according to NCBI (Table 3). Also, CapD is postulated to form homodimers and the residues involved are 314, 316, 320, 324, 339–342, 345, 348, 366–369, 372, 376, 379, 382, 453–454, and 459. Thus, it can be extrapolated that the amino acid sequences of lipase that are mapped to CapD residues responsible for homodimer formation are also most likely responsible for forming homodimers.

In all the microbial lipases, its interaction with the lipid interface is facilitated through the movement of a lid like α-helical structure near the lipase active site. Due to the lid movement, the lipase active site becomes fully exposed to the lipid, which eventually results in a hydrophobic interaction of lipase with the lipid substrate [2]. Interestingly, the MALDI-TOF-MS results did not map to the active site residues (Asn384, Thr408, Met418, Lys422 in CapD protein). However, we think that the C-terminus region is where the catalytic function resides. Also, the lipase from *S. arlettae* is thought to be a serine hydrolase [10]. Although, as seen in the inset of Fig. 3, there is a lid-like structure that is spatially closer to the α/β Rossmann domain, and it is most likely that this structural part has a functional role as observed in other microbial lipases. Among the six fragments obtained (residues Met2-Lys7, Arg68-Lys82, Arg162-Arg166, Lys304-Lys308, Arg349-Lys368, and Lys462-Arg479) two of them a map to the α/β Rossmann- fold domain. While, residues Arg349-Lys368 in Cap1D of *S. aureus* are responsible for the formation of homodimers, we think that these residues are important in *S. arlettae* JPBW-1 lipase to be a contributing factor for its homodimer formation, which most likely has a direct implication to its optimal activity. While Cap1D of *S. aureus* (599 residues) has a molecular weight of 67.57 kDa and in comparison *S. arlettae* JPBW-1 lipase (~410 residues) has a molecular weight of 45 kDa, we conclude that the C-terminus sequence of lipase most likely forms a α/β Rossmann fold domain with a lid as with other lipases that also fall under α/β class of proteins, and we conclude that the C-terminus of *S. arlettae* JPBW-1 lipase is where lies the most probable location for its active site.

For structural comparison, we took the lipase from *Chromobacterium viscosum* ATCC 6918 [20] as an example structure and compared it with the C-terminal domain of *S. aureus*'s CapD protein. Using combinatorial extension algorithm of PyMOL [21] the proteins were structurally superposed (Fig. 4), and we observed that *C. viscosum* lipase has four helices like the CapD protein. These helices with its connecting loops are spatially arranged above the active site region (Ser87, His285, and Asp263). This has been reported as the substrate binding domain consisting of five helices and two antiparallel β strands [21].

4 Concluding remarks

The three-step purification of *S. arlettae* JPBW-1 lipase (halo-, solvent-, detergent- and thermo-tolerant) has been reported here for the first time, which resulted in a 270-fold purification and having a molecular weight of 45 kDa. The amino acid sequence obtained through MALDI-TOF-MS revealed that they share significant similarity with CapD or Cap1D protein of *S. aureus*. A comparative modeling approach was performed for obtaining a 3D model for the CapD protein of *S. aureus* using ROBETTA server. MALDI-TOF/TOF-MS revealed amino acid sequences that were mapped to the 3D structure of CapD protein and we identified the involvement of two fragments in the protein, which possibly are involved in the homodimer formation. Moreover, by comparing the C-terminus of CapD with lipase from *Chromobacterium viscosum* we propose that a substrate binding domain (comprising of four helices) possibly facilitate the substrate binding and thereby initiating the catalytic reaction. Thus, coupled with experimental and molecular modeling studies we have postulated a relationship between structure and activity of lipase from *S. arlettae* JPBW-1.

Practical application

Present research put forth the purification and molecular modeling of a new unique lipase with halo-, solvent-, and thermo- tolerance. Responsible fragments for homodimer formation have been identified through comparative modeling and substrate binding domain through C-terminus matching of this new lipase with the capsular polysaccharide biosynthesis protein (CapD) of *Staphylococcus aureus*. The present experimental result coupled with molecular modeling postulated a structure–activity relationship of *Staphylococcus arlettae* JPBW-1 lipase as a probable catalyst for detergent, leather, pulp, and paper industries due to its halo-, solvent-, and thermo- tolerance.

The authors gratefully acknowledge JUIT, Himachal Pradesh, India for providing research fellowship to Mamta Chauhan, research facilities to Ragothaman M. Yennamalli.

The authors have declared no conflict of interest.

5 References

[1] Hasan, F., Shah, A. A., Hameed, A., Industrial applications of microbial lipases. *Enzyme Microb. Tech.* 2006, *39*, 235–251.
[2] Jaeger, K. E., Reetz, M. T., Microbial lipases form versatile tools for biotechnology. *Trends Biotechnol.* 1998, *16*, 396–403.
[3] Garlapati, V. K., Banerjee, R., Solvent-free synthesis of flavour esters through immobilized lipase mediated transesterification. *Enzyme Res.* 2013, *2013*, 367410.
[4] Shu, Z. Y., Jiang, H., Lin, R. F., Jiang, Y. M., Lin, L., Huang, J. Z., Technical methods to improve yield, activity and stability in the development of microbial lipases. *J. Mol. Catal. B: Enzym.* 2010, *62*, 1–8.
[5] Xiao, M., Mathew, S., Obbard, J. P., Biodiesel fuel production via transesterification of oils using lipase biocatalyst. *GCB Bioenerg.* 2009, *1*, 115–125.
[6] Bisen, P. S., Sanodiya, B. S., Thakur, G. S., Baghel, R. K., Prasad, G., Biodiesel production with special emphasis on lipase-catalyzed transesterification. *Biotechnol. Lett.* 2010, *32*, 1019–1030.
[7] Hasan, F, Shah, A. A., Javed, S., Hameed, A., Enzymes used in detergents: lipases. *Afr. J. Biotechnol.* 2010, *9*, 4836–4844.
[8] Basheer, S. M., Chellappan, S., Beena, P. S., Sukumaran, R. K., Elyas, K. K., Chandrasekaran, M., Lipase from marine *Aspergillus awamori* BTMFW032: Production, partial purification and application in oil effluent treatment. *New Biotechnol.* 2011, *28*, 627–638.
[9] Mhetras, N. C., Bastawde, K. B., Gokhale, D. V., Purification and characterization of acidic lipase from *Aspergillus niger* NCIM 1207. *Bioresour. Technol.* 2009, *100*, 1486–1490.
[10] Chauhan, M., Garlapati, V. K., Production and characterization of a halo-, solvent-, thermo tolerant alkaline lipase by *Staphylococcus arlettae* JPBW-1, isolated from rock salt mine. *Appl. Biochem. Biotechnol.* 2013, *171*, 1429–1443.
[11] Schwede T. Protein modeling: what happened to the "protein structure gap"? *Structure* 2013, *21*, 1531–1540.
[12] Garlapati, V. K., Banerjee, R., Evolutionary and swarm intelligence-based approaches for optimization of lipase extraction from fermented broth. *Eng. Life. Sci.*, 2010, *10*, 265–273.
[13] Lowry, O. J., Rosebrough, N. J., Farr, A. L., Randall, R.J., Protein measurement with the Folin phenol reagent. *J. Biol. Chem.* 1951, *193*, 265–275.
[14] Vijayakumar, K. R., Gowda, L. R., Lipase: Molecular cloning, functional expression and substrate specificity. *Protein Express. Purif.* 2013, *88*, 67–79.
[15] Laemmli, U.K., Cleavage of structural proteins during assembly of head of bacteriophage T4. *Nature* 1971, *227*, 680–685.
[16] Kim, D.E., Chivian, D., Baker, D., Protein structure prediction and analysis using the Robetta Server. *Nucleic Acids. Res.* 2004, *32*, W526–W531.
[17] Hio, A., Jonzo, A. D., Druet, D., Comeau, L., Production, purification and characterization of an extracellular lipase from *Mucor hiemalis f. hiemalis. Enzyme Microb. Technol.* 1999, *25*, 80–87.
[18] Xie, W., Khosasih, V., Suwanto, A., Kim, H.K., Characterization of lipases from *Staphylococcus aureus* and *Staphylococcus epidermidis* isolated from human facial sebaceous skin. *J. Microbiol. Biotechnol.* 2012, *22*, 84–91.
[19] Jones, D. T., Protein secondary structure prediction based on position-specific scoring matrices. *J. Mol. Biol.* 1999, *292*, 195–202.
[20] Lang, D., Hofmann, B., Haalck, L., Hecht, H. J., Spener, F., Schmid, R. D., Schomburg, D., Crystal structure of a bacterial lipase from *Chromobacterium viscosum* ATCC 6918 refined at 1.6Å resolution. *J. Mol. Biol.* 1996, *259*, 704–717.
[21] The PyMOL Molecular Graphics System, Version 1.8 Schrödinger, LLC.